Photonic crystal fibers with flattened zero dispersion for supercontinuum generation

Kokou Firmin Fiaboe[1], Pranaw Kumar[2 *] and Jibendu Sekhar Roy[3]

[1, 2,3] School of Electronics Engineering, KIIT University, Bhubaneswar , India
*corresponding author, E-mail: kumarpranaw9@gmail.com

Abstract

In this paper unique photonic crystal fiber (PCF) structure with nanoholes embedded have been studied. Embedded nanoholes have been filled with different materials of alcoholic groups like butanol, ethanol, methanol and propanol. Investigations of these structure shows flattened zero dispersion in visible range to far infrared regions. Simulated PCF structure reports ultra-low confinement loss of the order of 10^{-8} dB/km. Designed PCF promises to give large nonlinear coefficient of 3000 $W^{-1}Km^{-1}$ at 1335nm wavelengths. Numerical simulation of the fiber for the generation of supercontinuum generation (SCG) has been performed. Low power pump pulses of 50fs duration have been used. With a fiber of length of 15cm and pulses of 1kW, 2kW, 5kW and 10kW peak power, supercontinuum broadening of about 607nm, 908nm, 1987nm and 2405nm respectively.

1. Introduction

Supercontinuum generation is an inherent property of non-linear optics [1-2]. It is widely used in optical communication [3], pulse compression [4], spectroscopic meteorology [5] and coherence tomography [6]. SCG is a non -linear process which produces broadband light. This is achieved through the interaction of short and intense pulses which are output of narrow band sources and use nonlinear materials. Achieving a broadband supercontinuum generation in silica fibers has been a vital challenge for the researchers. The first requirement to achieve this is to obtain zero ultra-flattened dispersion PCFs. The nonlinear effects like Soliton phenomenon, Raman effect and Kerr effect are used for supercontinuum generation. This broadened the bandwidth of injected optical pulses. Dispersion regime of PCF strongly affects the non-linear behavior. Again in normal dispersion regime, a crucial role is being played by self-phased modulation for the broadening of pulses. Breaking of optical waves and intra-pulses raman scattering, for very short pulses result broad spectrum. The scalable periodic dielectric materials which are designed to affect the propagation of electromagnetic waves are termed as photonic crystals. Light manipulations like cavities and waveguides are done on the ability of photonic crystals to control wave propagation. These cavities and waveguides depends on two guiding mechanisms, modified total internal reflection and photonic band gap. Photonic crystal fibers (PCFs) proposed by Russell, due to its unusual properties like endless single mode propagation [7], large non-linear coefficient [8], high birefringence [9] and chromatic dispersion [10] make them, a point of attraction for the researchers. PCFs often termed as microstructured optical fiber are formed by single material with periodic arrangement of multiple air filled holes surrounding core. These microstructured fibers are divided into photonic band gap and index guiding fibers [11-12]. Index guiding PCFs utilizes modified total internal reflection. Index guiding PCFs form the core with the missing air holes. The air holes arranged periodically act as cladding for the fibers. These air holes create an average refractive index lower than the core. Hence it can be concluded that periodic distribution of air holes is not necessary which brings more flexibilities in designing PCFs. Flexibilities in designing PCFs make the fiber easy to achieve unique properties which cannot be observed in standard optical fibers. To mitigate or to minimize the effect of dispersion, zero dispersion PCFs or dispersion shifted fibers are designed with excellent results at different communication wavelengths. Due to flexibilities in designing of PCFs, several new PCF structures have come into picture. Researchers, utilizing these flexible parameters reported various PCF structures with flattened dispersion over a wide range of wavelength [13-15]. PCFs traditionally have hexagonal pattern surrounding the core. Recently, in order to achieve more significant results other arrangements like circular [16], square [17], rectangular [18], octagonal [19], decagonal [20] and dodecagonal [21] PCFs have also been investigated. Saitoh *et al* proposed a flattened dispersion PCF with triangular lattice [22]. Also Zhang *et al* investigated a square lattice PCFs [23]. Due to very small core diameters in PCFs, light propagates in single modes over a broad wavelength range. Hence, each passing coherent and short optical pulses with peak power through supercontinuum generation can be obtained in visible, near and mid-infrared regions. Supercontinuum generations have variety of applications in the field of optics. First, supercontinuum generations in PCF were demonstrated by Ranka *et al* [24]. After that various investigations have been made to reveal the mechanism behind supercontinuum generation. Supercontinuum spectra can be generated by pumping ultra-short pulses in fibers whose wavelength lies in dispersion regime close to zero dispersion wavelengths. Supercontinuum in PCFs have been studied with single zero

dispersion wavelength [25]. Also, enhance supercontinuum bandwidth with much flatness has also been obtained with two zero dispersion wavelengths [26-29]. PCFs with large nonlinear coefficient can be achieved by using silica and non-silica glasses. Razzak *et al* obtained a high nonlinear coefficient with octagonal PCF [30]. Further, Camerlingo *et al* proposed a W-type index profile lead silicate fiber with a nonlinear coefficient of $0.82W^{-1}m^{-1}$ at zero dispersion wavelengths of about 1550nm [31]. Till date various researchers have investigated nonlinear properties of PCF. For example, Saitoh *et al*, Dong *et al* and Finazzi *et al* have obtained nonlinear coefficient in range of 30 $W^{-1}Km^{-1}$ to 76 $W^{-1}Km^{-1}$ [32-34]. In similar fashion PCF can be easily tailor to result some unique feature [35-37].

In this work, simulation of PCF structure with embedded nanoholes, arranged in a hexagonal lattice have been done. These PCF structures have been doped with different materials of alcoholic groups (-OH groups). Materials of alcoholic groups like butanol, ethanol, methanol and propanol have been used as doping materials. One PCF structure with air filled holes has been investigated and results are compared with other PCF structures. All the five simulated PCF structures have resulted ultra-flattened zero dispersion. A very large nonlinear coefficient has been obtained with ultra-low confinement loss.

2. Design of nanoholes embedded PCF structures

Five PCF structures doped with materials of alcoholic groups were studied. PCF Structure is made such that nanoholes, doped with different materials are embedded in hexagonal lattice. Similarly, a PCF structure with air filled nanoholes is studied and results are compared. Schematic diagram of designed PCF structure have been shown in Fig. 1. Descriptions of proposed PCF structures are tabulated in Table-I.

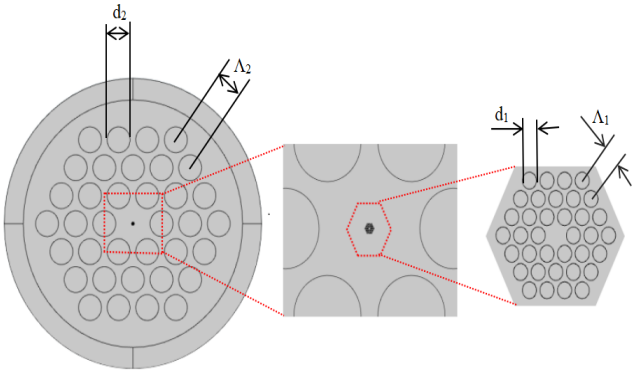

Figure 1: Designed PCF structure with inner hexagonal three ring having holes of diameter $d_1=0.8\Lambda_1$, where $\Lambda_1=0.05\mu m$. The external rings have three rings of holes with diameter $d_2=0.8\Lambda_2$, where $\Lambda_2=1.5\mu m$.

Table. I Description of simulated PCF structures

PCF Structures	**Descriptions**
Silica_Air	This structure has three rings of holes of circular dimension filled with air. At centre it has nanoholes arranged in hexagonal pattern filled with air. Nanoholes have diameter of $d_1=0.8\Lambda_1$, where $\Lambda_1=0.05\mu m$. External three rings have air holes of diameter $d_2=0.8\Lambda_2$, where $\Lambda_2=1.5\mu m$.
Silica_Butanol	This structure has three rings of holes of circular dimension filled with air. At centre it has nanoholes arranged in hexagonal pattern filled with butanol. Its refractive index is 1.3991. Nano holes have diameter of $d_1=0.8\Lambda_1$, where $\Lambda_1=0.05\mu m$. External three rings have air holes of diameter $d_2=0.8\Lambda_2$, where $\Lambda_2=1.5\mu m$.
Silica_Ethanol	This structure has three rings of holes of circular dimension filled with air. At centre it has nanoholes arranged in hexagonal pattern filled with Ethanol. Its refractive index is 1.36. Nanoholes have diameter of $d_1=0.8\Lambda_1$, where $\Lambda_1=0.05\mu m$. External three rings have air holes of diameter $d_2=0.8\Lambda_2$, where $\Lambda_2=1.5\mu m$.
Silica_Methanol	This structure has three rings of holes of circular dimension filled with air. At centre it has nanoholes arranged in hexagonal pattern filled with Methanol. Its refractive index is 1.327. nanoholes have diameter of $d_1=0.8\Lambda_1$, where $\Lambda_1=0.05\mu m$. External three rings have air holes of diameter $d_2=0.8\Lambda_2$, where $\Lambda_2=1.5\mu m$.
Silica_Propanol	This structure has three rings of holes of circular dimension filled with air. At centre it has nanoholes arranged in hexagonal pattern filled with Propanol. Its refractive index is 1.376. nanoholes have diameter of $d_1=0.8\Lambda_1$, where $\Lambda_1=0.05\mu m$. External three rings have air holes of diameter $d_2=0.8\Lambda_2$, where

	Λ_2=1.5μm.

Full vector finite element method (FEM) numerical technique has been adopted to analyse the different propagation characteristics of PCF. First FEM processes complex structured PCFs into homogeneous subspaces. Secondly, it is computed with Maxwell's vector equation as given by equation (1) and (2) [38].

$$\nabla*([s]^{-1}\nabla*E)-k_0^2n^2[s]E=0 \quad (1)$$

$$[s]=\begin{pmatrix} s_y/s_x & 0 & 0 \\ 0 & s_x/s_y & 0 \\ 0 & 0 & s_xs_y \end{pmatrix} \quad (2)$$

Where [s] is perfectly matched layer matrix of dimension 3X3. It includes even parameters S_x and S_y. Electric vector is denoted by 'E'. Wave number in vacuum is obtained as:

$$K_0=2\pi/\lambda \quad (3)$$

A circularly perfectly matched layer, boundary condition having thickness 10% of the fiber radius have been used to absorb the scattered light towards the surface of the fiber. Propagation constant (β) and effective refractive index at different wavelength (λ) are provided by the simulating software COMSOL Multiphysics 5.2. These are represented as:

$$\beta=n_{eff}K_0 \quad (4)$$

Dispersion of PCF is the total sum of waveguide dispersion and material dispersion [38].

$$D(\lambda)=D_w(\lambda)+D_M(\lambda) \quad (5)$$

Again, obtained effective refractive index of the guided fundamental modes at different wavelengths helps in calculating dispersion parameters of PCF by using the following mathematical expressions:

$$D_w(\lambda)=\frac{-2\pi c}{\lambda^2}\beta_2=\frac{-\lambda}{c}\frac{d^2n_{eff}}{d\lambda^2} \quad (6)$$

Material dispersion can be calculated as:

$$D_M(\lambda)=\frac{-\lambda}{c}\frac{d^2n_m}{d\lambda^2} \quad (7)$$

Here, n_m represents refractive index of material. It is derived from sellemier equation.

The cross sectional area of mode field, over which the field gets confined along the fiber during its propagation is termed as effective area. High optical intensities are the results of smaller effective area. Hence, PCF with small effective area results large nonlinear coefficient [39]

$$A_{eff}=(\int_{-\infty}^{\infty}\int_{-\infty}^{\infty}|E|^2\,dxdy)^2/\int_{-\infty}^{\infty}\int_{-\infty}^{\infty}|E|^4\,dxdy \quad (8)$$

$$\gamma=\frac{2\pi n_2}{A_{eff}\lambda} \quad (9)$$

Where $|E|$ is the transverse electric field.

$n_2=3.0\times10^{-20}m^2W^{-1}$, is the nonlinear refractive index of silica used. n_2 decides the degree to which nonlinear effects occur when light with high intensity propagate into the fiber.

Modes with leaky nature, together with non-perfect structure of PCFs result confinement loss. It is an extra form of loss which occurs in PCFs, usually made up of silica. These modes get leaky due to the finite lattice structure of PCFs. Confinement loss is calculated by considering imaginary part of the refractive index. It is calculated using formula [39]:

$$L\left(\frac{dB}{m}\right)=\frac{40\pi}{\ln(10)\lambda}\mathrm{Im}(n_{eff}) \quad =8.686K_0\,\mathrm{Im}[n_{eff}] \quad (10)$$

Normalized frequency or $V_{effective}$ of PCFs can be calculated as [34]:

$$V_{effective}=\frac{2\pi\Lambda}{\lambda}\sqrt{(n_{effective}^2-n_{co}^2)} \quad (11)$$

Where Λ is pitch factor. λ is corresponding wavelength. $n_{effective}$ and n_{core} are the modal index number and refractive index of core respectively.

Investigation of supercontinuum generation in the design fiber has been made. Modified nonlinear Schrodinger equation describes the mathematical model of supercontinuum generation. Schrodinger equation has different linear and nonlinear effects. This equation is solved using Split step Fourier method [40-42].

$$\frac{\partial}{\partial Z}A(Z,T)=\frac{-\alpha(\omega)}{2}A(Z,T)+\sum_{n\geq 2}\beta_n\frac{i^{n+1}}{n!}\frac{\partial^n}{\partial t^n}A(Z,T)$$
$$+i\gamma(1+\frac{i}{\omega_0}\frac{\partial}{\partial T})\int_{-\infty}^{\infty}R(T')\,|\,A(Z,T-T')\,|^2\,dT' \quad (12)$$

Where A (Z, T) represents slow varying envelope of the electric field of the optical pulse. The pulses move in a frame of reference along the z- direction at the pump frequency of the group velocity. α represent the attenuation constant of the fiber. β_n is the n^{th} order propagation constant at the center frequency ω_o. *R (T)* shows the nonlinear response function. It includes Raman contribution. It is defined as:

$$R(T)=(1-f_r)\delta(T)+f_r h_r(T) \quad (13)$$

f_r represent fractional contribution of the delay Raman response. Its value is taken to be 0.18. h_r represent form of Raman response function and it is calculated as

$$h_r(T)=\frac{\tau_1^2+\tau_2^2}{\tau_1\tau_2^2}\exp(-\frac{T}{\tau_2})\sin(\frac{-T}{\tau_1}) \quad (14)$$

Where τ_1=12.2*fs* and τ_2=32*fs* use for silica. Possibility of cross phase modulation between pulses of two different polarizations are minimized as the assume input pulse with either possess vertical or horizontal polarization during launching into the fiber.

3. Simulation and Results

PCF structure consists of embedded nanoholes arranged in hexagonal arrangements. Dimension of these nanoholes is $d_1=0.8\Lambda_1$. Here Λ_1 is the pitch factor and its value taken is 0.025µm. However, three ring hexagonal PCF, have air holes of diameter $d_2=0.8\Lambda_2$. Pitch factor (Λ_2) taken is 1.5µm. Designed PCFs have been simulated by finite element method (FEM) method of COMSOL Multiphysics 5.2 software.

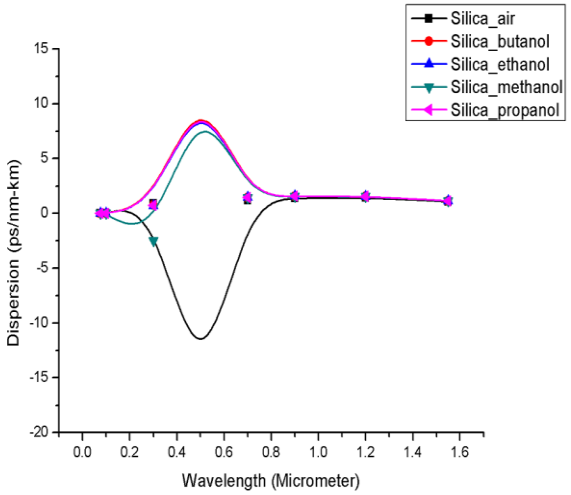

Figure 2: Dispersion behavior at different wavelengths

Air diameter of the inner most ring of PCF strongly determines its dispersion properties. Slope of waveguide dispersion compensate the slope of material dispersion in single mode PCF with smaller air hole diameter in the inner most ring [38-39]. Fig. 2 shows the dispersion behavior of all the five PCF structures simulated in this paper. Ultra flattened zero dispersion over visible range to far infrared region is obtained. Flattened zero dispersion over such a wide band of wavelength, is capable enough to make the nonlinear effects preponderant in these bands.

Diameter or dimension of holes in the cladding region, center to center spacing in between holes and number of air holes in the ring strongly affect confinement loss. Confinement loss increases with increase in wavelength. PCF structure doped with propanol in the nanoholes shows higher loss in comparison to other PCF structures. Similarly, butanol doped PCF structure reports the lowest confinement loss. Fig. 3 shows obtained confinement loss at each wavelength.

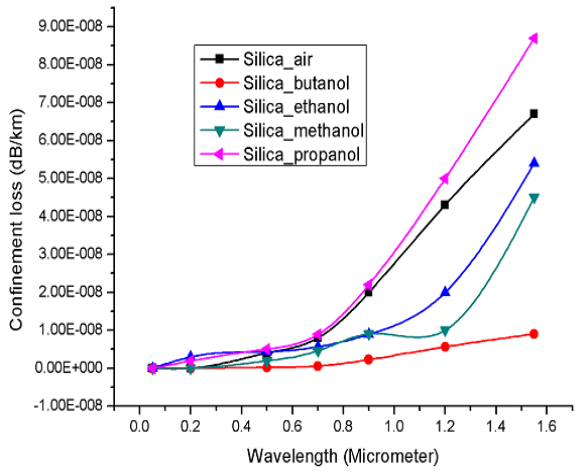

Figure 3: Confinement loss reported at different wavelengths

Effective mode area is inversely proportional to the non-

linear co-efficient. Effective mode area and its relation with the operating wavelength is shown in the Fig. 4. Similarly, non-linear co-efficient has also been reported in Fig. 5.

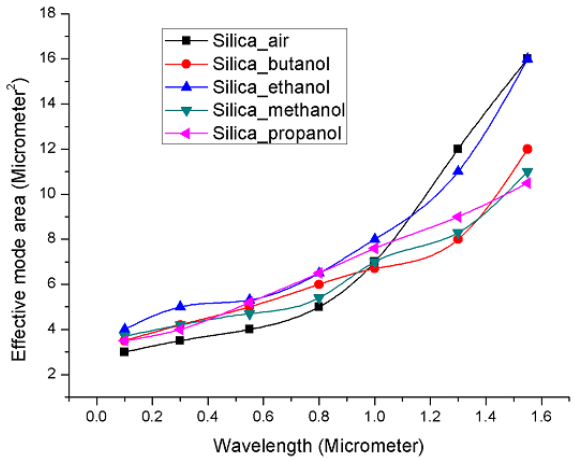

Figure 4: Effective mode area at different wavelengths

In designing single mode fiber size of fundamental mode plays a vital role. The same can be named as effective mode area. It relates to the effective area of the fiber core. Effective mode area, relevance to losses like bending loss, confinement loss and splice loss and numerical aperture is considered to be a significant parameter for studying modal characteristic. Large effective mode area is needed for the transmission of high power. Small mode area PCFs are preferred when desired to enhance nonlinear properties of fiber. In other words, effective mode area is a measuring parameter of nonlinear properties of fiber.

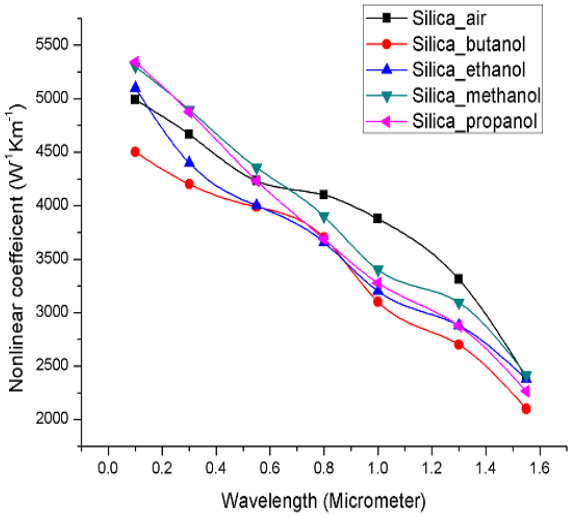

Figure 5: Nonlinear co efficient at different wavelengths

Normalized frequency decides single mode propagation of any photonic crystal fibers. Normalized frequency, also termed as $V_{effective}$ maintains a significant value of lesser or equal to 4.1, to determine single mode property of a PCF. Fig. 6 shows clearly that PCF structures studied in this work are endlessly single mode fibers.

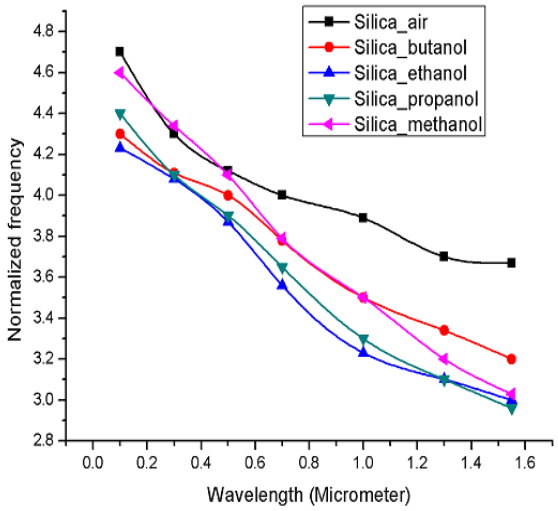

Figure 6: Normalized frequency

In this paper we explain supercontinuum generation with the help of PCF having length of 15 cm. Dispersion profile and zero dispersion wavelengths play a vital role in obtaining needed characteristic of supercontinuum generation. These characteristics include width and flatness. We have obtained zero dispersion over a wide band of wavelength, however pump pulses at 1335 nm has been used for simulation of supercontinuum generation. PCF has shown zero dispersion at this wavelength other values of different high order term of dispersion at 1335 nm are:

$\beta_2 = -8.767 ps^2/km$, $\beta_3 = 3.969\times10^{-3} ps^3/km$, $\beta_4 = -5.937\times10^{-6} ps^4/km$, $\beta_5 = 2.846\times10^{-9} ps^5/km$, $\beta_6 = -1.520\times10^{-12} ps^6/km$, $\beta_7 = 3.284\times10^{-15} ps^7/km$, $\beta_8 = -7.489\times10^{-17} ps^8/km$, $\beta_9 = 2.689\times10^{-20} ps^9/km$ and $\beta_{10} = -8.909\times10^{-22} ps^{10}/km$.

Ultra short laser pulses with hyperbolic secant shape are introduced as the input to the PCF. These pulses equation can be characterized as:

$$U(0,T) = \sqrt{P_o}\,\mathrm{sech}\left(\frac{T}{T_o}\right) \quad (15)$$

Where T_0 represents the temporal width of input pulse. Higher order soliton become some dominant phenomena in the case of ultra-short pulses pumped into zero dispersion regime [40-41]. Soliton number determines these high order solitons. It can be calculated as

$$N^2 = L_D / L_{NL} \quad (16)$$

Here L_D represent dispersion length and it is equal to

$L_D = T_0^2 / |\beta_2|$. Similarly $L_{NL} = 1/\gamma P_0$ where L_{NL} is the nonlinear length . P_0 is the peak power used, β_2 is the group velocity dispersion coefficient. In Fig. 7, soliton numbers for the generation of supercontinuum are calculated against the variation of input pulse duration. It reveals that decrease in the duration of the input pulse leads to the generation of more number of high order soliton. Calculated soliton number are very large at the given peak power.

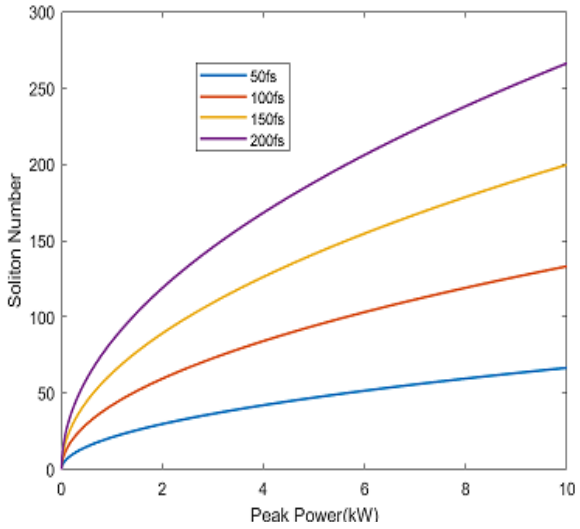

Figure 7: Number of solitons generated at different input pulses

Such a large generation of soliton may cause intra soliton interaction. Again dispersion length calculated is found to be 55 cm. It shows much larger fiber than the actual fiber length of 15 cm. Dispersion effect degrade in comparison to the nonlinear terms. Nonlinear effect determines the pulse evolution and result spectral broadening of these pulses. Effect of pulse compression are affected by soliton fission length. These length are calculated using $L_{fiss} = L_D / N$. The calculated value has been plotted in Fig. 8. Small duration of pulses causes in early pulse compression. It results smaller fission length and hence result wide spectrum.

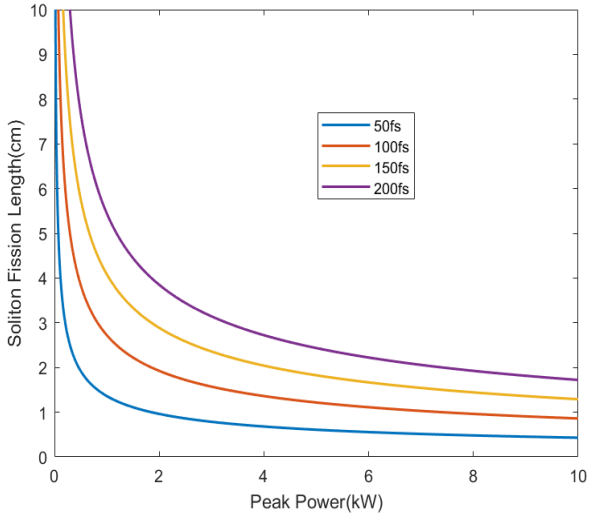

Figure 8: Soliton fission length at different input pulses

Optical pulse of 50 fs duration at 1335nm as pumping pulse of supercontinnum generation has been utilized. Numerical simulation for supercontinuum generation has been done at four different peak power levels 1kW, 2kW, 5kW and 10 kW in the PCF structure with air holes. Fiber loss, being very low, is therefore neglected for short length of PCF. It is further expected that loss will not affect supercontinuum generation. Firstly, numerical simulations for supercontinuum generation for different fiber length by using pulse of 1kW power have been performed. Fig. 9 (a) represent the spectral evolution of the input pulse for five different length of fiber respectively. More information about spectra broadening dynamic may be capture by displaying the broadening phenomenon, using a density plot. In this plot the spectral intensity has been plotted using logarithmic density scale shorter at -40dB relative to maximum value. The density plot is displayed in Fig. 9 (b). This plot is utilized for studying the low amplitude spectral and temporal components.

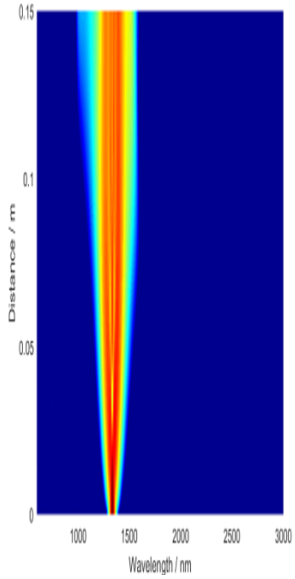

Fig. 9 (a)

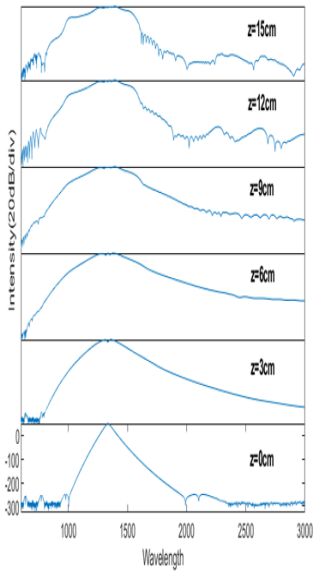

Fig. 9 (b)

Figure 9: Density plot of spectral profile Fig. 9 (a) and Spectral profile Fig. 9(b) of supercontinuum generation of a 15cm long silica PCF at peak power of 1kW with pulses of 50fs duration

Modulation instability dominates the spectral broadening initially. Later, it is dominated by self-phase modulation (SPM), four wave mixing, Raman scattering and Dispersive wave generation. The spectrum at the end is 607nm wide. Similarly, we increase the peak power to 2kW, 5kW and 10kW respectively to simulate supercontinuum generation. With the increase in the input peak power of the pulse , we are getting a wider broadening at the output of the fiber .The spectral dynamic have been shown in Fig. 10 (a), Fig. 10 (b), Fig. 11 (a), Fig. 11 (b), Fig. 12 (a) and Fig. 12 (b) respectively. The supercontinuum spectra for peak power 1kW, 5kW and 10kW are 607nm, 908nm, 1987nm and 2405nm respectively.

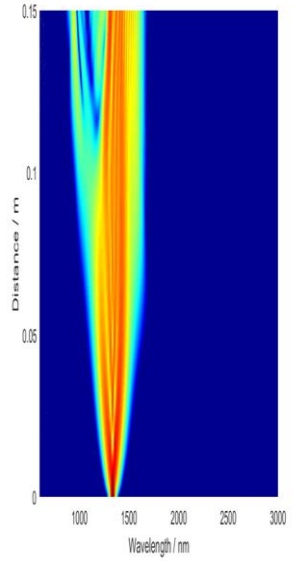

Fig. 10 (a)

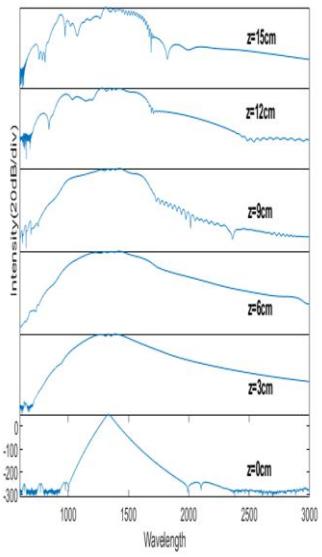

Fig. 10 (b)

Figure 10: Density plot of spectral profile Fig. 10 (a) and Spectral profile Fig. 10(b) of supercontinuum generation of a 15cm long silica PCF at peak power of 2kW with pulses of 50fs duration.

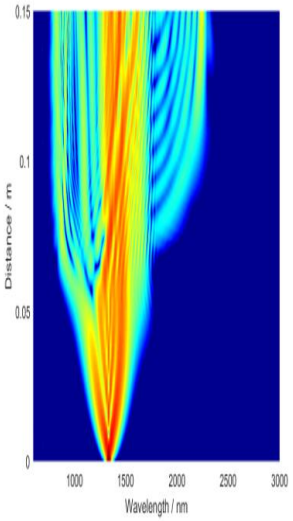

Fig. 11 (a)

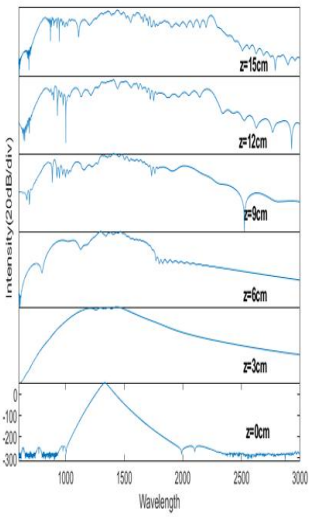

Fig. 11 (b)

Figure 11: Density plot of spectral profile Fig. 11 (a) and Spectral profile Fig. 11(b) of supercontinuum generation of a 15cm long silica PCF at peak power of 5kW with pulses of 50fs duration

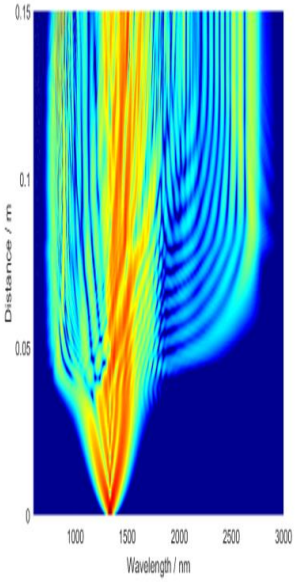

Fig. 12 (a)

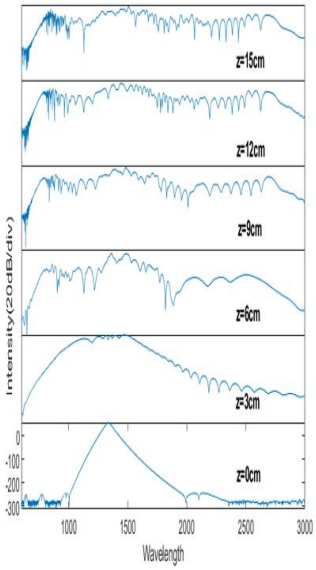

Fig. 12 (b)

Figure 12: Density plot of spectral profile Fig. 12 (a) and Spectral profile Fig. 12(b) of supercontinuum

generation of a 15cm long silica PCF at peak power of 10kW with pulses of 50fs duration

Results obtained in this paper are compared with the previously reported results of PCF structures at the wavelength 1.33μm. This comparison is tabulated in Table II.

Table II: Comparison with the previously reported PCF structures at 1.33μm wavelength

References	Dispersion	Effective mode area	Nonlinear coefficient
[42]	50ps/nm-km	0.7 μm^2	300 $W^{-1}Km^{-1}$
[47]	100ps/nm-km	4.3 μm^2	50 $W^{-1}Km^{-1}$
[48]	30ps/nm-km	4.3 μm^2	50 $W^{-1}Km^{-1}$
[49]	170ps/nm-km	-------	2000 $W^{-1}Km^{-1}$
Present work	Flattened zero	14 μm^2	3000 $W^{-1}Km^{-1}$

4. Conclusions

A highly nonlinear hexagonal PCF, containing embedded three rings of nanoholes have been studied. Embedded nano holes in PCF structures have been arranged in hexagonal lattice arrangements. Designed PCFs have shown ultra-flattened zero dispersion over the visible range to far infrared region. Due to this (zero dispersion) and large optical nonlinearity, designed fiber can be a capable medium for supercontinnum generation. A 15cm length of this PCF yield broadening of supercontinnum generation of about 2405nm with a pulse of 10kW. Number of solitons generated is large. Moreover, ultra-low confinement loss has been reported by the designed PCFs. Study of normalized frequency also confirms the designed PCF to be endless single mode. Infine, the designed PCF can be used in optical communication system with high rate of transmission, biomedical field and optical coherence tomography.

References

[1] J C. Knight, T. A. Birks, P. Russell, D. M. Atkin,"All-silica single mode optical fiber photonic crystal cladding", *Optics letters,* vol. 21, pp.1547-1551, 1996.

[2] M. Dudley. G. Genty, S. Coen, "Supercontinuum generation in photonic crystal fiber", *Rev. Mod. Phys*, vol. 78, issue-4, pp. 1135-1141, 2006.

[3] M. Sharma, N. Borogohain, and S. Konar, "Index guiding photonic crystal fibers with large birefringence and walk-off", *IEEE J. Lightwave Technol*. vol. 31, pp. 3339-3344, 2013.

[4] O. V. Shulika et al., "Characterization of all-normal-dispersion microstructured optical fiber via numerical simulation of passive nonlinear pulse reshaping and single-pulse flat-top supercontiuum", *J. Nanophotonics* vol. 8, pp. 83-89, 2014.

[5] H. Saghaei, M. Ebnali-Heidari, M. K. Moravvej-Farshi, "Mid infrared supercontinuum generation via As2Se3 chalcogenide photonic crystal fibers", *Appl. Opt.,* vol. 54, issue-8, pp. 2072-2079, 2015.

[6] V.Q. Nguyen, J.S. Sanghera, F. H. Kung, I. D. Aggarwal, I. K. Lloyd, "Effect of temperature on the absorption loss of chalcogenide glass fibers", *Appl. Opt.,* vol. 38, issue-15, pp.3206-3213, 1999.

[7] T. A. Birks, J. C. Knight, P. St, J. Russell, "Endlessly single-mode photonic crystal fiber", *Opt. Lett.* Vol. 22, pp. 961-963, 1997.

[8] X. Freng, et al., "Single-Mode tellurite glass holey fibre with extremely large mode area for nonlinear applications", *Opt. Express,* vol. 16 (18), pp.13651-13655, 2008.

[9] G. K. M. Hasanuzzaman, S. Rana, M. S. Habib, "A novel low loss, highly birefringent photonic crystal fiber in THz regime", *IEEE Photon. Technol. Lett.,* vol. 28, issue-8, pp. 899-902, 2016.

[10] K.P. Hansen, "Dispersion flattened hybrid-core non-linear photonic crystal fiber", *Opt. Express* vol. 11, pp.1503-1509, 2003.

[11] J. Wang, C. Jiang, W. Hu, M. Gao, "Properties of index guided PCF with air core", *Opt. Laser Technol.*, vol. 39, pp. 317-321, 2006.

[12] J. C. Knight, J. Broeng, T.A. Birks, P.St.J. Russell, "Photonic band gap guidance in optical fibers", *Science,* vol. 282 pp. 1476-1478, 1998.

[13] A. Ferrando, E. Silvestre, P. Andres, "Nearly zero ultra-flattened dispersion in photonic crystal fibers," *Opt. Lett.*, vol. 25, pp.790-792, 2000.

[14] F. Poletti, V. Finazzi, T. M. Monro, N. G. R. Broderick, V. Tse, D.J. Richardson, "Inverse design and fabrication tolerances of ultra-flattened dispersion holey fibers", *Opt. Express,* vol. 13, pp. 3728 – 3736, 2005.

[15] T. L Wu, C. H. Chao, "A novel ultra-flattened Dispersion Photonic Crystal fibers", IEEE *Photon. Technol. Lett.,* vol. 17, pp. 67-69, 2005.

[16] P. Kumar, V. Kumar, J. S. Roy, "Design of quad core photonic crystal fiber with flatteneed zero dispersion", International Journal of Electronics Communicationtios (AEU), Vol. 98, pp. 265-272, Nov. 2018.

[17] X. Lei, "Highly nonlinear with low confinement losses square photonic crystal fiber based on a four-hole unit", *Infrared Phy. Technol.,* vol. 66, pp. 29-33, 2014.

[18] G. Jiang, Y. F, Y. Haung, "High birefringence rectangular-hole photonic crystal fiber", Optical Fiber Technology, vol. 26, part B, pp. 163-171, Dec., 2015.

[19] J-S Chiang, T-L Wu, "Analysis of propagation characteristics for an octagonal photonic crystal fiber (O-PCF)", *Opt. Comm.* Vol. 258, 2006.

[20] S. M. A. Razzak, Y. Namihira, F. Begum, S. Kaijage, N. Zou, "Design of a decagonal photonic crystal fiber with ultra-Flattened chromatic dispersion", *IEICE Trans. Electron.,* E89-C (6), pp. 830-837, 2006.

[21] P. Kumar, Rohan, V. Kumar, J. S. Roy, "Dodecagonal photonic crystal fibers with negative dispersion and low confinement loss," *Optik* vol. 144, pp. 363-369, 2017.

[22] K. Saitoh, N. Florous, and M. Koshiba, "Ultra-flattened chromatic dispersion controllability using a defected-core photonic crystal fiber with low confinement losses," *Opt. Express*, vol. 13, pp. 8365-8371, 2005.

[23] M. Zhang, F. Zhang, Z. Zhang, and X. Chen, "Dispersion ultra-flattened square-lattice photonic crystal fiber with small

effective mode area and low confinement loss," *Optik,* vol. 125, pp. 1610-1614, 2014.
[24] J. K. Ranka, R. S. Windeler, A. J. Stentz, "Visible continuum generation in air-silica microstructure optical fibers with anomalous dispersion at 800 nm," *Opt. Lett.* Vol. 25, pp. 25-27, 2000.
[25] P. A. Anderson, C. Peucheret, K. Hiligose, K. S. Berg, K. P. Hasen, P. Jeppesen, "Supercontinuum generation in a photonic crystal fiber using picosecond pulses at 1550nm", *ICTON/ESPC'03*, pp. 66-69, 2003.
[26] A. Hartung, A. M. Heidt and H. Bartelt, "Design of all normal dispersion microstructured optical fibers for pulse preserving supercontinuum generation", *Opt. Express*, vol. 19, pp. 7742-7749, 2011.
[27] A. Aguirre, N. Nishizawa, J. G. Fujomoto, W. Seitz, M. Lederer, D. Kopf, "Continuum generation in a novel photonic crystal fiber for ultrahigh resolution optical coherence tomography at 800nm and 1300nm", *Opt. Express,* vol. 14, pp. 1145-1160, 2006.
[28] A.Mandilara, C. Valagiannopoulos, and V. M. Akulin, "Classical and quantum dispersion-free coherent propagation by tailoring multimodal coupling" *Physical review*, vol. 99, pp. 02349(1)-02349(8), 2019.
[29] Ming-Jun Li ; D. A. Nolan, "Optical Transmission Fiber Design Evolution", *Journal of Lightwave Technology* , vol. 26 ,no. 9, pp. 1079-1092, May 2008.
[30] S. M. Abdur Razzak, Yoshinori Namihira, "Proposal for highly nonlinear dispersion flattened octagonal photonic crystal fibers", *IEEE Photonics Technol. Lett.,* vol. 20(4), pp.249-251, 2008.
[31] A. Camerlingo, X. Feng, F. Poletti, G.M. Ponzo, F. Parmigiani, P. Horak, M.N. Petrovich, P. Petropoulos, W. H. Loh, D.J. Richardson "Near-zero dispersion highly nonlinear lead-silicate W-type fiber for application at 1.55um", *Opt. Exp.* vol. 18(15), pp.15747-15756, 2010.
[32] K. Saitoh and M. Koshiba, "Highly nonlinear dispersion-flattened photonic crystal fibers for supercontinuum generation in a telecommunication window," *Opt. Express,* vol. 12, pp. 2027-2032, 2004.
[33] L. Dong, B. K. Thomas, and L. Fu, "Highly nonlinear silica suspended core fibers," *Opt. Express, vol.* 16, 16423-16430.
[34] V. Finazzi, T.M. Monro, and D.J. Richardson, "Small-core silica suspended core fibers: nonlinearity and confinement loss trade-offs", J. *Opt. Soc. Am. B* , vol. 20, pp. 1427-1436, 2003.
[35] C. Valagiannopoulos and P. G. Lagoudakis , "Photonic crystals for optimal color conversion in light-emitting diodes: a semi-analytical approach", *Journal of the Optical Society of America B*, Vol. 35, no. 5, pp. 1105-1112, 2018.
[36] R. Bhattacharya and S. Konar, "Design of a Photonic Crystal Fiber with Zero Dispersion Wavelength Near 0.65 μm", *Fiber and Integrated Optics*, vol. 27, pp. 89–98, 2008.
[37] A. Yu. Petrov and M. Eich , "Zero dispersion at small group velocities in photonic crystal waveguides ", *Appl. Phys. Lett*. , vol. 85, pp. 4866-4868, 2004.
[38] F. Poli, A. Cucinotta, S. Selleri, "Photonic crytal fibers properties and applications", *Springer series in materail sciences*, 2007.
[39] A. Ghatak, K. Thyagarajan, "Introduction to Fiber optics", *1st South Asian Edition* 1999.
[40] J. D. Joannopoulos, Steven G. Johnson, Josgua N. Winn, Robert D. Mede, Photonic crystal fiber: Molding the flow of light, 2nd edition, *Priceton University Press*, 2008.
[41] J. M. Dudely, J. R. Tylor,"Supercontinuum generation in optical fibers", *Cambridge University Press,* Cambridge, UK, 2010.
[42] M. sharma, S. Konar, R. K. khan,"Supercontinuum generation in highly nonlinear hexagonal photonic crystal fiber at very low power", *Journal of Nanophotonics,* vol. 9, pp.1-8, 2015.
[43] A. H. Bouk, A. Cucinotta, F. Poli, S. Selleri, "Dispersion properties of square-lattice photonic crystal fibers", *Opt. Express*, vol. 12, pp. 941-946, 2004.
[44] F. Poletti, V. Finazzi, T. M. Monro, N. G. Brodreick, V. Tse, D. J. Richardson,"Inverse design and fabrication tolerances of ultra-flattened dispersion holey fibers", *Opt. Express*, vol. 13, pp. 3728-3736, 2005.
[45] G. P. Agrawal, "Nonlinear Fiber Optics", (*Academic Press*, 2011).
[46] M. Sharma, S. Konar, "Three octave spanning supercontinuum by red-shifted dispers wave in photonic crystal fibers", *Journal of Modern Optics*, pp. 1-10, 2015.
[47] G. D. Kirishna, G. Prasanan, S. K. Sudheer, V. P. M. Pillai, "Analysis of zero dispersion shift and supercontinuum generation near IR in circular photonic crystal fibers", *Optik*, vol. 145, pp. 599-607, 2017.
[48] M. L. Ferhat, L. Cherbi, I. Haddouche, "Supercontinnum generation in silica photonic crystal fiber at 1.3μm and 1.65μm wavelength for optical coherence tomography", *Optik*, vol. 152, pp. 106-115, 2018.
[49] M. Sharma, S. Konar, "Broadband supercontinuum generationin lead silicate photonic crystal fibers employing optical pulses of 50W peak powers", *Optics Communication,* vol. 380, pp. 310-319, 2016.